Published in final edited form as:
J Neurochem. 2006 October ; 99(2): 549–560. doi:10.1111/j.1471-4159.2006.04087.x.

Ultrastructural localisation and differential agonist-induced regulation of AMPA and kainate receptors present at the presynaptic active zone and postsynaptic density

Marco Feligioni, **David Holman**, **Camilla Haglerod**[*], **Svend Davanger**[*], and **Jeremy M. Henley**
MRC Centre for Synaptic Plasticity, Department of Anatomy, School of Medical Sciences, University of Bristol, Bristol, UK

[*]Department of Anatomy and Centre for Molecular Biology and Neuroscience, University of Oslo, Blindern, Oslo, Norway

Abstract

Activity-dependent changes in ionotropic glutamate receptors at the postsynaptic membrane are well established and this regulation plays a central role in the expression of synaptic plasticity. However, very little is known about the distributions and regulation of ionotropic receptors at presynaptic sites. To determine if presynaptic receptors are subject to similar regulatory processes we investigated the localisation and modulation of AMPA (GluR1, GluR2, GluR3) and kainate (GluR6/7, KA2) receptor subunits by ultrasynaptic separation and immunoblot analysis of rat brain synaptosomes. All of the subunits were enriched in the postsynaptic fraction but were also present in the presynaptic and non-synaptic synaptosome fractions. AMPA stimulation resulted in a marked decrease in postsynaptic GluR2 and GluR3 subunits, but an increase in GluR6/7. Conversely, GluR2 and GluR3 increased in the presynaptic fraction whereas GluR6/7 decreased. There were no significant changes in any of the compartments for GluR1. NMDA treatment decreased postsynaptic GluR1, GluR2 and GluR6/7 but increased presynaptic levels of these subunits. NMDA treatment did not evoke changes in GluR3 localisation. Our results demonstrate that presynaptic and postsynaptic subunits are regulated in opposite directions by AMPA and NMDA stimulation.

Keywords

AMPA; kainate; synaptosomes; post-synaptic; pre-synaptic; regulation

In the mammalian CNS, fast excitatory synaptic neurotransmission is mainly mediated by AMPA receptors (AMPARs) whereas the closely related kainate receptors (KARs) play important roles in the regulation of both excitatory and inhibitory neurotransmission. Both receptor types are involved in the mechanisms underlying synaptic plasticity and their dysfunction has been implicated in neurodegenerative diseases (for reviews see Isaac *et al*. 2004; Palmer *et al*. 2005; Lerma 2006). Mature AMPARs and KARs are tetrameric assemblies. AMPARs can be made up of different combinations of four subunits: GluR1, GluR2, GluR3 and GluR4 (Hollmann and Heinemann 1994; Bettler and Mulle 1995). There are five KAR subunits in mammalian brain. KA1 and KA2 bind kainate with high affinity

Please address correspondence and reprint requests to Professor Jeremy M. Henley, Department of Anatomy and MRC Centre for Synaptic Plasticity, School of Medical Sciences, University of Bristol, Bristol BS8 1TD, UK. j.m.henley@bris.ac.uk.

but do not form functional homomeric channels. Instead they modify the properties of other subunits when co-expressed in heteromeric receptors. Subunits GluR5–7 bind kainate at lower affinity but can form functional homomeric channels (Chittajallu *et al.* 1999; Lerma *et al.* 2001).

The synaptic location of AMPARs and KARs is dictated by the equilibrium between insertion, removal and lateral diffusion of plasma membrane receptors and these highly regulated processes depend on neuronal activity (Bredt and Nicoll 2003; Lerma 2003). While it has been accepted for many years that KARs have important pre- and postsynaptic distributions and functions (Kullmann 2001; Lerma 2003; Jaskolski *et al.* 2005), presynaptic AMPARs have been largely overlooked. This is partly because studies using immunogold electron microscopy have been interpreted to suggest that AMPARs are exclusively postsynaptic (Ottersen and Landsend 1997). However, multiple lines of evidence now indicate that AMPARs are localised presynaptically and that these receptors can modulate synaptosomal glutamate release (Barnes *et al.* 1994; Patel and Croucher 1997; Rammes *et al.* 1998; Ghersi *et al.* 2003; Pinheiro *et al.* 2003; Schenk *et al.* 2003; Schenk and Matteoli 2004). Furthermore, it has recently been demonstrated that modulation of presynaptic AMPAR trafficking events, by disrupting GluR2 interactions with known trafficking partners, can significantly alter AMPAR-mediated neurotransmitter release (Pittaluga *et al.* 2006). Nonetheless, little is known about the regulation, composition and trafficking of presynaptic receptors and how this compares with the more extensively studied postsynaptic AMPAR and KARs.

The aim of this study was to investigate the ultrasynaptic localisation of AMPAR and KAR subunits under basal conditions and assess and compare pre- and postsynaptic changes evoked by AMPA or NMDA stimulation. We used a synaptic purification technique (Phillips *et al.* 2001; Pinheiro *et al.* 2003, 2005) to simultaneously analyse the presynaptic (active zone region), postsynaptic (PSD) and also non-synaptic synaptosomal protein of AMPAR and KAR subunits under basal and stimulated conditions. We define non-synaptic synaptosomal protein (NSSP) as all other synaptosomal protein including cytosolic protein in the sealed presynaptic bouton (and sometimes postsynaptic spine) and all membranes, including intracellular organelles, other than the active zone and PSD (Fig. 1). Our results show that individual subunits have differential distributions in each of these compartments indicative of the different receptor subunit assemblies. Furthermore, presynaptic and postsynaptic receptors are regulated in opposite directions in response to AMPA or NMDA stimulation of the synaptosomes prior to isolation of the fractions. These data demonstrate that AMPAR and KARs are differentially regulated at different synaptic locations, most likely by their subunit-specific interactions with defined binding protein partners in the different compartments.

Materials and methods

Synaptosome preparation

To collect sufficient tissue for reliable and consistent ultrasynaptic purification we prepared synaptosomes from the pooled cortex and hippocampi from three Wistar adult rats (200–250 g). From ~3 g of starting tissue we obtained 0.2–0.8 mg of protein per ultrasynaptic fraction. The whole brains were frozen at −80°C in 10 m_M Tris buffer (pH 7.4 at 4°C) containing 0.32 $_M$ sucrose. When needed, the tissue was dissected to obtain cortex and hippocampi and thawed and homogenised in 24 mL of the same buffer (4°C; pH 7.4) containing standard protease inhibitors (Complete EDTA-free; Roche Molecular Biochemicals, Indianapolis, IN, USA). The resultant homogenate was centrifuged at 1000 *g* for 5 min to remove nuclei and cellular debris. Synaptosomal fractions were purified by centrifugation for 5 min at 33 500 *g* using Percoll-sucrose density gradient (2–6–10–20%; v/v). The synaptosomal fraction from

the 10–20% Percoll interface (Nakamura *et al.* 1993) was collected, washed to eliminate Percoll and used as the starting material for subsequent experiments.

Synaptosome stimulation

Synaptosomes were resuspended in 1.2 mL HEPES buffer (mM): NaCl, 140; KCl, 3; $MgSO_4$, 1.2; $CaCl_2$, 1.2; NaH_2PO_4, 1; $NaHCO_3$, 5; glucose, 10; HEPES, 5; pH 7.4 and then divided in to 0.6-mL aliquots and gently agitated at 37°C. After 8 min of agitation, antagonist or vehicle was added to the synaptosome suspensions. After a further 6 min, agonist or vehicle was added and the suspensions incubated for 6 min. For all conditions after a total incubation time of 20 min, 0.6 mL of ice-cold medium was added the suspension was immediately centrifuged at 16 000 *g* to collect the synaptosomes. For NMDA stimulation experiments Mg^{2+} was omitted to avoid the functional inactivation of the receptor.

Ultrastructural fractionation

The synaptosome pellets were resuspended in 300 μL HEPES buffer (4°C; pH 7.4) and 50 μL was removed and kept as a total. Synaptosomes were pelleted by centrifugation (16 000 *g*; 5 min; 4°C) and resuspended in 300 μL 0.32 M sucrose and 0.1 mM $CaCl_2$. Protease inhibitors were used in all extraction steps. Synaptosomes were then diluted 1 : 10 in ice-cold 0.1 mM $CaCl_2$ and mixed with an equal volume of 2× solubilisation buffer (2% Triton X-100, 40 mM Tris, pH 6.0; 4°C). Following 30 min incubation at 4°C the insoluble material (synaptic junctions; Phillips *et al.* 2001) was pelleted by centrifugation (40 000 *g*, 30 min, 4°C). The supernatant (NSSP) was decanted and proteins precipitated with 6 volumes of acetone at −20°C and centrifuged (18 000 *g*; 30 min; − 15°C). The synaptic junction pellet was resuspended in 10 volumes of 1 × solubilisation buffer (1% Triton X-100, 20 mM Tris, pH 8.0; 4°C) and incubated for 30 min at 4°C and then centrifuged (40 000 *g*, 30 min, 4°C). The pellet contained the insoluble postsynaptic density and the supernatant contained the presynaptic active zone. The protein in the supernatant (presynaptic fraction) was acetone precipitated and collected as above. A schematic of the synaptic fractionation protocol is shown in Fig. 1.

Electron microscopy

For electron microscopy, synaptosomes and ultrasynaptic fractions were fixed as pellets overnight in 1.0% formaldehyde and 2.5% glutaraldehyde in sodium phosphate buffer, pH 7.4. The pellets were subsequently stored in sodium phosphate buffer containing 0.1% formaldehyde and 0.25% glutaraldehyde. Before embedding in Durcupan® (ACM Fluka, Buchs, Germany) the pellets were treated with 1.0% OsO_4 in 0.1 M sodium phosphate buffer for 30 min and dehydrated in graded ethanols and propylene oxide. Ultrathin sections were cut and contrasted with 5% uranyl acetate for 90 s, and with 2.66% lead citrate for 90 s. The ultrathin sections were observed in a Tecnai Philips CM12 electron microscope.

Slice preparation

Slices 400 μm thick were prepared from cortex and hippocampi of adult Wistar rats in ice-cold artificial cerebrospinal fluid (composition in mM: 124 NaCl; 3 KCl; 26 $NaHCO_3$; 1.25 NaH_2PO_4; 2 $CaCl_2$; 1 $MgSO_4$; 10 D-glucose; saturated with 95% oxygen and 5% carbon dioxide). Slices were transferred to a submersion storage chamber where they were maintained in artificial CSF for 1 h at room temperature.

Slice biotinylation

Slices were washed once with ice-cold artificial CSF (5 min) and then incubated with NHS-SS-Biotin (Pierce, Rochford, IL, USA; 0.5 mg/mL in artificial CSF) for 30 min on ice. Excess biotin was removed by two brief washes with 50 mM NH_4Cl (in artificial CSF)

followed by two further artificial CSF washes. Slices were then homogenised in 1 mL of homogenisation buffer (320 mM sucrose; 10 mM Tris; pH 7.4; 4°C) and synaptosomes were prepared.

Solubilisation of synaptosomes prepared from biotinylated slices

Purified synaptosomes prepared from biotinylated slices were resuspended in 1 mL of lysis buffer (150 mM NaCl; 20 mM HEPES; 2 mM EDTA; 1% Triton; 0.1% SDS; pH 7.4 at 0°C), sonicated and placed on a head-over-head shaker for 2 h at 4°C to allow a maximum solubilisation of biotinylated and non-biotinylated proteins prior to the streptavidin pull-down protocol. Protein assays were performed using Pierce BCA kit.

Streptavidin pull-down

Streptavidin beads (30 μL; Sigma, St Louis, MO, USA) were washed three times with lysis buffer. Lysed biotinylated samples were added to the beads (60 μg total protein) and mixed for at least 4 h. Beads were centrifuged at 800 *g* and supernatants removed. The supernatants (unbound fraction) were used to determinate the intracellular expression of receptor subunits. Beads were then washed three times with lysis buffer and biotinylated proteins were eluted using 2× loading buffer at 90°C for 5 min.

SDS-PAGE and western blots

Samples of 30 μL corresponding to 12 μg of protein were resolved using 8% or 10% sodium dodecyl sulfate–polyacrylamide gel electrophoresis (SDS-PAGE) denaturing gels run at 120 V. Proteins were transferred to polyvinylidene fluoride (PVDF) membrane using a semidry blotting system for 75 min at 15 V. After transfer, nonspecific binding sites were blocked overnight with Tris-buffered saline-Tween (t-TBS; 0.02 M Tris, 0.137 M NaCl, and 0.1% Tween 20) containing 5% non-fat dried milk. The PVDF membranes were then probed with primary antibodies for 90 min at room temperature. The primary antibodies and dilutions used were: mouse anti-PSD95, 1 : 1000 (Upstate Biotechnology, Lake Placid, NY, USA); mouse anti-Syntaxin, 1 : 10000 (Sigma); mouse anti-Synaptophysin, 1 : 20000 (Calbiochem, San Diego, CA, USA), goat anti-PICK1, 1 : 1500 (SantaCruz, Santa Cruz, CA, USA); rabbit anti-GluR1, 1 : 1500 (Upstate); mouse anti-GluR2, 1 : 1500 (Chemicon, Temecula, CA, USA); mouse anti-GluR3, 1 : 500 (Chemicon); rabbit anti-GluR6/7, 1: 2000 (Upstate); rabbit anti-KA2, 1 : 1000 (Upstate); mouse antiβ-tubulin, 1 : 4000 (Sigma); mouse anti-N-cadherin, 1, 2000 (BD Transduction Laboratories, San Diego, CA, USA). Membranes were then washed three times with t-TBS and incubated for 2 h at room temperature with the appropriate horseradish peroxidase-linked secondary antibody: anti-goat, 1 : 5000 (Sigma); anti-mouse, 1 : 5000 (Amersham Bioscience Inc., Piscataway, NJ, USA) or anti-rabbit, 1 : 10 000 (Amersham Bioscience). After a further three washes with t-TBS, immunoreactive bands were detected by the chemiluminescence detection system enhanced chemiluminescence western blot analysis system (Roche). The immunoreactive bands were visualised by exposure to Hyperfilm MP (Amersham Biosciences).

Semiquantitative immunoblotting

Western blots were quantified by densitometric analysis using NIH IMAGE J software. For biotinylation experiments, defined amounts (15, 30 and 60 μg) of total protein were resolved alongside the streptavidin bound and unbound fractions. Following western blot analysis, optical density values were obtained for each of the bands representing the input, bound and unbound fractions. By plotting these values the percentage surface expression of each subunit was determined by normalising the unbound optical band density value to the input band density values. We used the streptavidin bead unbound bands instead of the bound

Europe PMC Funders Author Manuscripts

bands to avoid potential error due to incomplete elution efficiency from the biotin-streptavidin complex.

Results

Electron microscope characterisation of ultrasynaptic fractions

We assessed the structures present in the pre-, post- and NSSP fractions by electron microscopy (Fig. 2). As expected, the total brain homogenate (Figs 2a, b) contains a multiple different structures including synapses (Fig. 2b), mitochondria and nuclei. In the enriched synaptosome fraction nearly all the synaptosomes had sealed presynaptic membrane structures (Figs 2c–e). A minority also had sealed postsynaptic membrane structures (Fig. 2d) whereas the majority had open postsynaptic membrane structures (Fig. 2e). Following the initial detergent extraction, extrasynaptic membrane was solubilised. The purified postsynaptic fraction (Figs 2f, g) consists of semidense, amorphous matter. Small, slightly curved dark ‘rods’ are present that we interpret as partly intact PSDs. In addition, in some places the amorphous matter contains grey or black granules that are sometimes densely accumulated as black spots. These are proteins most likely originating from disintegrated PSDs. The presynaptic fraction (Figs 2h, i) contains a loose array of small, grey spots. They are clearly larger than the small granules in the postsynaptic purified fraction. At higher magnification, many of them are identified as vesicular and we interpret these as aggregated proteins associated with small presynaptic vesicles with the active zone. There are also some larger vacuolar-like structures, as well as some intermediate, dark structures that may be large dense core granules. The NSSP fraction comprises detergent solubilised protein that was subsequently precipitated with acetone. The micrographs (Figs 2j, k) show granular precipitates consisting of all of the cytosolic and membrane protein other than that directly incorporated in, or strongly associated with, the active zone or postsynaptic density.

Biochemical characterisation of fractions

We next investigated the distribution of well characterised marker proteins in the purified fractions (Fig. 3). Consistent with the structures in the electron microscope profiles and with previous reports (Phillips *et al.* 2001; Pinheiro *et al.* 2003) PSD95 was predominant in the postsynaptic fraction with only a low level detected in the presynaptic fraction (Fig. 3a). Similarly, the presynaptic membrane protein syntaxin (Kasai and Akagawa 2001) was highly enriched in the presynaptic fraction (Fig. 3b). In both cases there was little or no cross-contamination between the fractions. As expected, the synaptic vesicle membrane protein synaptophysin was highly abundant in the NSSP fraction. Synaptophysin was also present, although to a much lesser extent, in the presynaptic fraction, which we attribute to vesicles docked to the active zone of the presynaptic membrane (Richmond and Broadie 2002). PICK1 has both pre- and postsynaptic roles (Hirbec *et al.* 2002) and consistent with this it was distributed in each of the fractions.

Extent of AMPAR/KAR surface expression in synaptosomes

To define the fraction of receptor surface expression in synaptosome surface proteins in resting, non-stimulated brain slices were biotinylated prior to the preparation of synaptosomes. This avoided labelling of intracellular proteins that would occur due to leaky or unsealed synaptosomes (Thomas-Crusells *et al.* 2003). Following synaptosome preparation, surface expressed proteins were isolated by streptavidin pull-down and resolved by semiquantitative western blots (Fig. 4). Between 65% and 80% of each of GluR1-GluR3 and KA2 subunits were surface expressed in synaptosomes, whereas ~40% of GluR6/7 was present at the surface. The intracellular protein β-tubulin was used as a control. Occasionally, an extremely weak β-tubulin band was discernible that we attribute to biotin

access to cells unavoidably damaged during the slice preparation. However, the fact that β-tubulin was present overwhelmingly in the unbound fraction indicated that only surface proteins were biotinylated. N-cadherin, which plays a key role in cell–cell adhesion processes, is localised at the cell surface at the synaptic active zone and in intracellular compartments (Yamagata *et al.* 2003). Thus, the fact that N-cadherin was abundant in the streptavidin-retained fraction confirmed that surface expressed proteins within the synaptic cleft are efficiently biotinylated.

Ultrasynaptic distribution of AMPAR and KAR subunits

Under non-stimulated conditions, all of the AMPAR and KAR subunits tested were most abundant in the postsynaptic density fraction but the relative proportions varied for the different subunits (Fig. 5). Similarly, all of the subunits were present in the presynaptic fraction, indicating that AMPAR and KARs are located within the synaptic cleft at the presynaptic active zone. There was considerable subunit variability in the amount of immunoreactivity in the NSSP fraction. Of the AMPAR subunits, GluR1 was relatively abundant in the NSSP fraction (~ 20%) with comparatively similar proportions (35–45%) present in the pre- and postsynaptic fractions. Only very low levels of GluR2 were detected in the NSSP fraction with ~60% post- and ~35% presynaptic. GluR3 was not detected in the NSSP fraction. The presence of GluR1 in NSSP fraction suggests that either homomeric GluR1 or receptors containing mainly GluR1 with low levels of GluR2 (or possibly GluR4) are present in presynaptic vesicles. The KAR subunits GluR6/7 and KA2 were predominantly present in the PSD (~ 80%) with much lower levels of presynaptic and NSSP fractions present. This is consistent with immunogold electron microscope studies showing a mainly postsynaptic localisation for KA2 (Darstein *et al.* 2003).

AMPA stimulation evokes differential changes in pre- and postsynaptic subunit distributions

We next investigated the effect of AMPA application to synaptosomes for 6 min at 37°C (Fig. 6, Table 1). No effects were observed in the presence of the antagonist CNQX. Markedly different AMPA-evoked changes were observed for the individual subunits which were blocked by inclusion of 10 μ_M NBQX (data not shown). GluR1 levels were unchanged in any of the fractions by incubation with 50 μ_M AMPA. In contrast, GluR2 and GluR3 were slightly but significantly decreased at the postsynaptic density and dramatically increased in the presynaptic fraction. The similarity in the profile of changes for GluR2 and GluR3 are consistent with these two subunits residing in the same receptor complex. In the NSSP fraction, only GluR2 is significantly changed, consistent with the internalisation of GluR2 containing AMPARs from the presynaptic membrane to intrasynaptosomal locations.

AMPA also evoked large changes in KAR subunits, presumably via KA2-containing KARs that bind AMPA as an agonist and/or membrane depolarisation. Interestingly, in direct contrast to AMPAR subunits, GluR6/7 was increased in the postsynaptic and decreased in the presynaptic fractions. NSSP vesicular GluR6/7 is also decreased by AMPA, consistent with the presynaptic degradation of these subunits rather than their redistribution to intracellular membranes or to presynaptic membranes outside the active zone. The profile for KA2 differed from GluR6/7. This subunit was unchanged in the postsynaptic, decreased in the presynaptic and very markedly increased in the NSSP fractions.

NMDA receptor activation results in a different profile of subunit distribution

In hippocampal slices, transient NMDA receptor activation leads to a form of long-term depression (chem-LTD (Lee *et al.* 1998)) and postsynaptic AMPARs are removed from synapses following NMDA exposure in cultured neurones (Beattie *et al.* 2000; Ashby *et al.* 2004). We therefore tested the effects of NMDA treatment on synaptosomes prior to

separation of the synaptic compartments. No effects were observed in the presence of the antagonist APV. There were differential effects on the AMPAR and KAR subunits (Fig. 7, Table 1). All NMDA-evoked changes were completely prevented by inclusion of 10 μM AP5 (data not shown).

In common with previously reported postsynaptic AMPAR internalisation, the postsynaptic fractions GluR1 and GluR2 were significantly decreased. The reduction in GluR1 and GluR2 is consistent with these subunits existing in heteromeric complexes that are regulated by synaptic activation. In the presynaptic active zone fractions GluR1 and GluR2 were both significantly increased by NMDA application. In the NSSP fraction GluR1 was dramatically increased and so, to a lesser extent, was GluR2. This is consistent with the redistribution of subunits away from the PSD either laterally in the membrane or into intracellular compartments. There was no significant change in GluR3 in any of the fractions.

Discussion

Here we report the proportions of receptor subunits present in enriched synaptic membrane fractions under basal and stimulated conditions. We demonstrate the effective separation of presynaptic and postsynaptic membranes using previously validated markers. Furthermore, the presence of the non-integral membrane protein PICK1 in the active zone and PSD fractions indicates that membrane-associated proteins could also be copurified. Taken together, these data indicate that successful separation of pre- and postsynaptic compartments was achieved. The nature of the NSSP fraction is less defined as it contains membrane and cytosolic proteins present in synaptosomes that are not in, or tightly associated with, the active zone or PSD.

There is one brief report comparing the pre- and postsynaptic distributions of AMPAR subunits (Pinheiro *et al.* 2003) and one for KAR subunits (Pinheiro *et al.* 2005). Both those studies investigated only basal, non-stimulated, conditions. Using GluR1–GluR4 antibodies those workers found relatively similar levels at pre-, post- and extrasynaptic membranes from synaptosomes. We also found strong presynaptic AMPAR immunoreactivity but our data differ in that we observed marked differential compartmentalisation. For KAR subunits we observed similar distributions for GluR6/7 and KA2 subunits but other anti-KAR antibodies were not reliable in our hands.

We determined the extent of surface expressed receptors under basal conditions by biotinylating slices prior to preparation of the synaptosomes. Our values are higher than the 30–50% reported for surface expression in the entire neurone (for review see (De La Rue and Henley 2002)) consistent with the fact that surface functional AMPARs and KARs are targeted to and clustered at synapses. Because of the unavoidably low yield, despite pooling hippocampi and cortex, it was not feasible to investigate the surface expression in each of the individual ultrasynaptic fractions. However, as the pre- and postsynaptic fractions comprise solely active zone or PSD, we conclude that the percentage surface expression in these fractions is greater than that measured for synaptosomes overall. The NSSP fraction arises from all of the intracellular synaptosomal membranes (vesicles, endoplasmic reticulum, etc.) as well as non-synaptic synaptosomal plasma membrane. Thus, the proportion of surface expressed receptors in this fraction is likely much lower. Based on these observations, we propose that changes in receptor abundance in the pre- and postsynaptic fractions predominantly represent changes in surface expressed, functionally relevant subunits.

AMPAR and KAR subunits were most abundant in the PSD fraction but were also present in the presynaptic active zone fraction. The proportion in the NSSP fraction varied, probably

reflecting the fact that synaptosomes originated from many different types of hippocampal and cortical synapses. Nonetheless, the ultrasynaptic distributions are consistent with previous studies suggesting that AMPAR subunits are present in synaptic vesicles and that these can be recruited to the presynaptic membrane as functional receptors in response to KCl-evoked depolarisation (Schenk *et al.* 2003) and with immunogold electron microscopy showing a mainly postsynaptic localisation for KA2 (Darstein *et al.* 2003).

Our results indicate that AMPA stimulation evokes differential changes in pre- and postsynaptic subunit distributions. It has been proposed that GluR1/GluR2 complexes are driven into synapses during long-term potentiation (LTP), whereas GluR2/GluR3 complexes are constitutively inserted regardless of synaptic activity (Shi *et al.* 2001). At the presynaptic terminal it has been reported that GluR1 and GluR2 are actively internalized upon activation and recruited to the surface upon depolarisation (Schenk *et al.* 2003). We observe down-regulation of postsynaptic AMPAR at the PSD consistent with agonistinduced internalisation and degradation (Ehlers 2000; Lee *et al.* 2004) but suggest an up-regulation of presynaptic GluR2/GluR3 containing AMPARs close to the neurotransmitter release sites in the active zone. The reasons for this are unclear but it is possible that presynaptic AMPARs, like presynaptic KARs, could act as sensors to decrease neurotransmitter release. On the other hand, this increase in presynaptic AMPARs might act as a positive feedback mechanism to sensitise the synapse and enhance subsequent release events.

For KARs we interpret the AMPAR-evoked changes in subunit distribution to suggest that, to a large extent. GluR6/7 and KA2 occur in different receptor assemblies and that the KA2-containing receptors are likely internalised from the presynaptic membrane (both in the active zone and outside it) to presynaptic vesicles. As shown in Fig. 5, KA2 is mainly postsynaptic and it has been reported that KA1 is largely presynaptic (Darstein *et al.* 2003). Although the fraction of surface expressed GluR6/7 appears markedly lower than KA2, it is not possible to compare the intensity of immunoreactive bands obtained using different antibodies. Thus, even though the GluR6/7 band is faint it does not mean that there is not sufficient expression to drive KA2 to the surface. Unfortunately, there are not currently any reliable anti-GluR5 antibodies so we cannot directly test the distribution of this subunit.

Different subunits distribution profiles were observed following NMDA receptor activation. As expected from chem-LTD experiments, NMDA evokes a decrease in GluR1 and GluR2 levels in the PSD whereas GluR1, GluR2 and GluR6/7 subunit-containing receptors are recruited to the presynaptic active zone following NMDA stimulation. This may be due to the docking of receptor-containing neurotransmitter vesicles or stabilisation of receptors in the active zone that otherwise would have been removed and degraded. Overall, our results suggest that GluR1/GluR2 assemblies (containing more GluR1 than GluR2) are subject to regulation and that GluR3 (probably in GluR2/GluR3 assemblies) are relatively unaffected. Interestingly, the KAR subunits GluR6/7 and KA2 show opposite NMDA response profiles to each other. Postsynaptic and NSSP GluR6/7 is significantly decreased whereas KA2 is significantly increased and *vice versa* at the presynaptic membrane. As for the AMPA stimulation, one possible explanation for these results is that the changes in KARs are attributable to GluR6/7 in assemblies with KA1 and KA2 in assemblies with GluR5.

There are several considerations that should be noted in the interpretation of these data. First, pre- and postsynaptic intracellular membranes and plasma membrane outside the synapse (i.e. not active zone or PSD) is solubilised during the fractionation procedure and all the protein partitions to the NSSP fraction. Second, due to the limitations of semiquantitative western blot analysis, which requires two different antibody binding steps, it is not possible to calculate the absolute amounts of subunits in each fraction. Rather, the results are presented as a percentage of the sum of the three fractions. It is apparent from the protein-

matched western blots the postsynaptic fraction is always more enriched in subunits than the presynaptic fraction, which, in turn, is more enriched than the NSSP fraction. Furthermore, in some cases the immunoreactive bands are close to detection limits so changes must be interpreted with caution because of the potential influence of background noise. Third, it is not possible directly to resolve surface expressed from membrane-associated proteins in the ultrasynaptic fractions. For example the postsynaptic fraction comprises the PSD and a proportion of subunits detected are also likely to correspond to receptors anchored by interacting proteins at the internal face of the PSD within the spine. We did, however, measure surface expression in synaptosomes and these data indicate that in excess of 70% of the subunits present are at the surface. Notwithstanding these unavoidable technical limitations, our data show for the first time that drug application to synaptosomes results in differential changes in ultrasynaptic subunit expression.

Consistent with data from cultured hippocampal cultures (Ehlers 2000; Lee *et al.* 2004) showing that the fate of internalised postsynaptic AMPARs differs depending on the stimulation protocol, we observed different ultrasynaptic distribution profiles evoked by AMPA and NMDA. Similar to the situation for AMPARs, internalised KARs are also sorted into recycling or degradative pathways depending on the endocytotic stimulus. Kainate activation causes internalisation of KARs that are targeted to lysosomes for degradation, whereas NMDA receptor activation evokes endocytosis of KARs to early endosomes with subsequent re-insertion into the plasma membrane (Martin and Henley 2004). Perhaps most strikingly, GluR1 distribution was not altered by AMPA, whereas GluR3 was significantly changed in both pre- and postsynaptic fractions. The reverse was observed following NMDA application: GluR3 was unaffected but there were dramatic changes in GluR1. GluR2 was changed by both AMPA and NMDA, suggesting that this subunit is present in most receptor assemblies.

In conclusion, we show, for the first time, simultaneous and opposite AMPA or NMDA-evoked changes in the presynaptic and postsynaptic compartments that indicate the presence of complex and dynamic regulatory processes to control the levels of AMPARs and KARs at distinct ultrasynaptic sites. The fact that pre- and postsynaptic receptors are regulated in different directions by the same stimulus raises intriguing questions as to the physiological consequences for synaptic transmission and plasticity.

Acknowledgments

We are grateful to the MRC, the Wellcome Trust and the EU (GRIPANNT, PL 005320) for financial support. We thank Fred Jaskolski, Stéphen Martin, Tristan Bouschet, Peter Hastie and Jon Hanley for useful advice and constructive criticism of the manuscript.

Abbreviations used

AMPAR	AMPA receptor
Ka	kainate
KAR	kainate receptor
LTD	long-term depression
LTP	long-term potentiation
NSSP	non-synaptic synaptosomal protein
PSD	post-synaptic density
PVDF	polyvinylidene fluoride membrane

SDS-PAGE sodium dodecyl sulfate – polyacrylamide gel electrophoresis

References

Ashby MC, De La Rue SA, Ralph GS, Uney J, Collingridge GL, Henley JM. Removal of AMPA receptors (AMPARs) from synapses is preceded by transient endocytosis of extrasynaptic AMPARs. J. Neurosci. 2004; 24:5172–5176. [PubMed: 15175386]

Barnes JM, Dev KK, Henley JM. Cyclothiazide unmasks AMPA-evoked stimulation of [H-3]-L-glutamate release from rat hippocampal synaptosomes. Br. J. Pharmacol. 1994; 113:339–341. [PubMed: 7530567]

Beattie EC, Carroll RC, Yu X, Morishita W, Yasuda H, von Zastrow M, Malenka RC. Regulation of AMPA receptor endocytosis by a signaling mechanism shared with LTD. Nat. Neurosci. 2000; 3:1291–1300. [PubMed: 11100150]

Bettler B, Mulle C. AMPA and kainate receptors. Neuropharmacology. 1995; 34:123–140. [PubMed: 7542368]

Bredt DS, Nicoll RA. AMPA receptor trafficking at excitatory synapses. Neuron. 2003; 40:361–379. [PubMed: 14556714]

Chittajallu R, Braithwaite SP, Clarke VRJ, Henley JM. Kainate receptors: subunits, synaptic localisation and function. Tips. 1999; 20:544–553.

Darstein M, Petralia RS, Swanson GT, Wenthold RJ, Heinemann SF. Distribution of kainate receptor subunits at hippocampal mossy fiber synapses. J. Neuroscience. 2003; 23:8013–8019.

De La Rue SA, Henley JM. Proteins involved in the trafficking and functional synaptic expression of AMPA and KA receptors. ScientificWorldJournal. 2002; 2:461–482. [PubMed: 12806030]

Ehlers MD. Reinsertion or degradation of AMPA receptors determined by activity-dependent endocytic sorting. Neuron. 2000; 28:511–525. [PubMed: 11144360]

Ghersi C, Bonfanti A, Manzari B, Feligioni M, Raiteri M, Pittaluga A. Pharmacological heterogeneity of release-regulating presynaptic AMPA/kainate receptors in the rat brain: study with receptor antagonists. Neurochem. Int. 2003; 42:283–292. [PubMed: 12470701]

Hirbec H, Perestenko O, Nishimune A, Meyer G, Nakanishi S, Henley JM, Dev KK. The PDZ proteins PICK1, GRIP, and syntenin bind multiple glutamate receptor subtypes: analysis of PDZ binding motifs. J. Biol. Chem. 2002; 277(15):221–15. 224.

Hollmann M, Heinemann S. Cloned glutamate receptors. Annu. Rev. Neuroscience. 1994; 17:31–108.

Isaac JTR, Mellor J, Hurtado D, Roche K. Kainate receptor trafficking: physiological roles and molecular mechanisms. Pharmacol. Ther. 2004; 104:163–172. [PubMed: 15556673]

Jaskolski F, Coussen F, Mulle C. Subcellular localization and trafficking of kainate receptors. Trends Pharmacol. Sci. 2005; 26:20–26. [PubMed: 15629201]

Kasai K, Akagawa K. Roles of the cytoplasmic and transmembrane domains of syntaxins in intracellular localization and trafficking. J. Cell Sci. 2001; 114:3115–3124. [PubMed: 11590238]

Kullmann DM. Presynaptic kainate receptors in the hippocampus: slowly emerging from obscurity. Neuron. 2001; 32:561–564. [PubMed: 11719198]

Lee HK, Kameyama K, Huganir RL, Bear MF. NMDA induces long-term synaptic depression and dephosphorylation of the GluR1 subunit of AMPA receptors in hippocampus. Neuron. 1998; 21:1151–1162. [PubMed: 9856470]

Lee SH, Simonetta A, Sheng M. Subunit rules governing the sorting of internalized AMPA receptors in hippocampal neurons. Neuron. 2004; 43:221–236. [PubMed: 15260958]

Lerma J. Roles and rules of kainate receptors in synaptic transmission. Nat. Rev. Neurosci. 2003; 4:481–495. [PubMed: 12778120]

Lerma J. Kainate receptor physiology. Curr. Opin. Pharmacol. 2006; 6:1–9.

Lerma J, Paternain AV, Rodriguez-Moreno A, Lopez-Garcia JC. Molecular physiology of kainate receptors. Physiol. Rev. 2001; 81:971–998. [PubMed: 11427689]

Martin S, Henley JM. Activity-dependent endocytic sorting of kainate receptors to recycling or degradation pathways. EMBO J. 2004; 23:4749–4759. [PubMed: 15549132]

Nakamura Y, Iga K, Shibata T, Shudo M, Kataoka K. Glial plasmalemmal vesicles – a subcellular fraction from rat hippocampal homogenate distinct from synaptosomes. Glia. 1993; 9:48–56. [PubMed: 7902337]

Ottersen OP, Landsend AS. Organization of glutamate receptors at the synapse. Eur J. Neurosci. 1997; 9:2219–2224. [PubMed: 9464917]

Palmer CL, Cotton L, Henley JM. The molecular pharmacology and cell biology of {alpha}-amino-3-hydroxy-5-methyl-4-isoxazolepropionic acid receptors. Pharmacol. Rev. 2005; 57:253–277. [PubMed: 15914469]

Patel DR, Croucher MJ. Evidence for a role of presynaptic AMPA receptors in the control of neuronal glutamate release in the rat forebrain. Eur. J. Pharmacol. 1997; 332:143–151. [PubMed: 9286615]

Phillips GR, Huang JK, Wang Y, et al. The presynaptic particle web: ultrastructure, composition, dissolution, and reconstitution. Neuron. 2001; 32:63–77. [PubMed: 11604139]

Pinheiro PS, Rodrigues RJ, Rebola N, Xapelli S, Oliveira CR, Malva JO. Presynaptic kainate receptors are localized close to release sites in rat hippocampal synapses. Neurochem. Int. 2005; 47:309–316. [PubMed: 16005547]

Pinheiro PS, Rodrigues RJ, Silva AP, Cunha RA, Oliveira CR, Malva JO. Solubilization and immunological identification of presynaptic alpha-amino-3-hydroxy-5-methyl-4-isoxazolepropionic acid receptors in the rat hippocampus. Neurosci. Lett. 2003; 336:97–100. [PubMed: 12499049]

Pittaluga A, Feligioni M, Longordo F, Luccini E, Raiteri M. Trafficking of presynaptic AMPA receptors mediating neurotransmitter release: Neuronal selectivity and relationships with sensitivity to cyclothiazide. Neuropharmacology. 2006; 50:286–296. [PubMed: 16242162]

Rammes G, Swandulla D, Spielmanns P, Parsons CG. Interactions of GYKI 52466 and NBQX with cyclothiazide at AMPA receptors: experiments with outside-out patches and EPSCs in hippocampal neurones. Neuropharmacology. 1998; 37:1299–1320. [PubMed: 9849667]

Richmond JE, Broadie KS. The synaptic vesicle cycle: exocytosis and endocytosis in Drosophila and C. elegans. Curr. Opin. Neurobiol. 2002; 12:499–507. [PubMed: 12367628]

Schenk U, Matteoli M. Presynaptic AMPA receptors: more than just ion channels? Biol. Cell. 2004; 96:257–260. [PubMed: 15145529]

Schenk U, Verderio C, Benfenati F, Matteoli M. Regulated delivery of AMPA receptor subunits to the presynaptic membrane. EMBO J. 2003; 22:558–568. [PubMed: 12554656]

Shi S, Hayashi Y, Esteban JA, Malinow R. Subunit-specific rules governing ampa receptor trafficking to synapses in hippocampal pyramidal neurons. Cell. 2001; 105:331–343. [PubMed: 11348590]

Thomas-Crusells J, Vieira A, Saarma M, Rivera C. A novel method for monitoring surface membrane trafficking on hippocampal acute slice preparation. J. Neurosci. Methods. 2003; 125:159–166. [PubMed: 12763242]

Yamagata M, Sanes JR, Weiner JA. Synaptic adhesion molecules. Curr. Opin. Cell Biol. 2003; 15:621–632. [PubMed: 14519398]

Europe PMC Funders Author Manuscripts

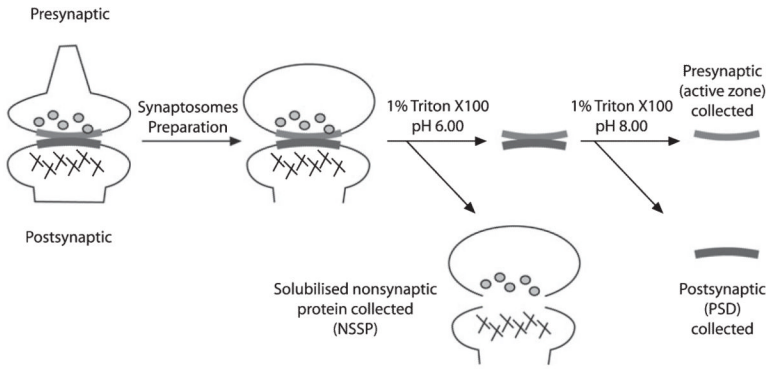

Fig. 1.

Schematic of the ultrasynaptic purification. Sequential solubilisation and centrifugation at pH 6.0 and 8.0 separate synaptic junctions and then pre- and postsynaptic compartments (Phillips *et al.* 2001). Note that all synaptosomal proteins not integral to or tightly associated with the presynaptic active zone (light grey) or the postsynaptic density (black) are solubilised and partition to the NSSP fraction.

Europe PMC Funders Author Manuscripts

Europe PMC Funders Author Manuscripts

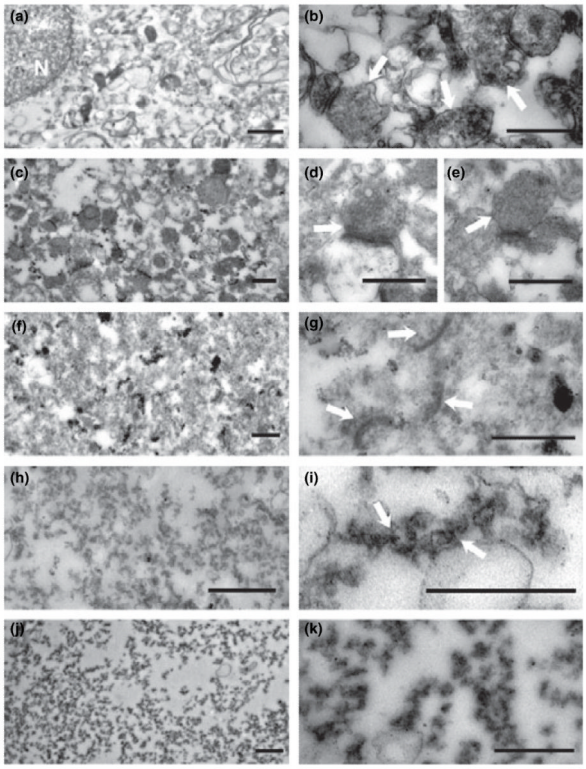

Fig. 2.

Electron microscope analysis of ultrasynaptic fractions. Synaptosomes from the cortex + hippocampus were subjected to ultrasynaptic separation and imaged by electron microscopy. (a) Total brain homogenate. (b) Crude synaptosome fraction. (c) Enriched synaptosomes showing synaptosomes with both sealed pre- and postsynaptic membranes (d) and sealed presynaptic and open postsynaptic membranes (e). (f, g) Purified postsynaptic fraction. (h, i) Purified presynaptic fraction. (j, k) NSSP fraction. The scale bars are: a, h, j, k: 1 μm and b, c, d, e, f, g, i: 0.5 μm.

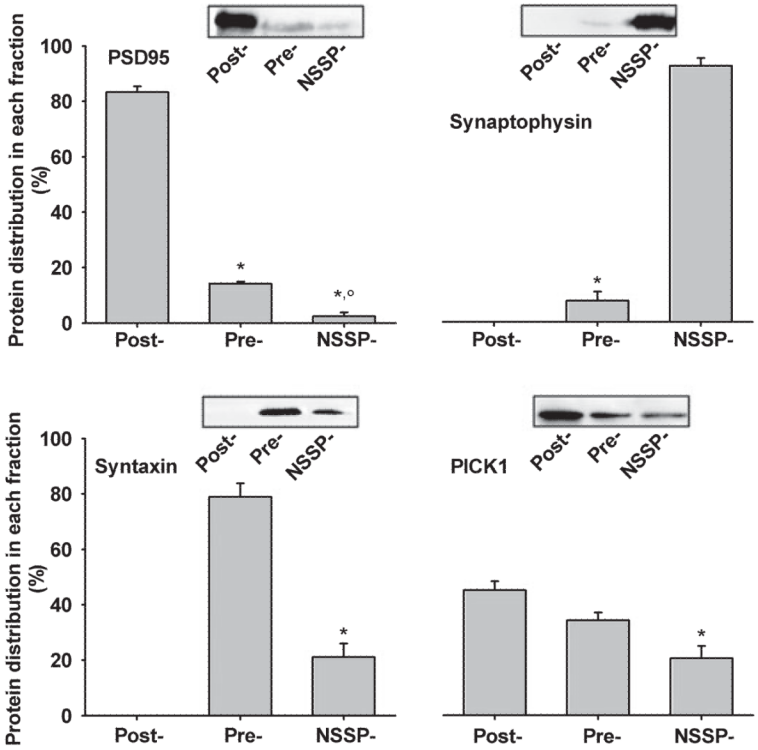

Fig. 3.

Validation of ultrasynaptic compartments using marker proteins: Aliquots of each ultrasynaptic fraction (12 μg/lane) were probed with antibodies against the well-characterised pre- and postsynaptic proteins shown. Quantitative analysis of the distributions is expressed as mean ± SEM ($n = 3$ separate immunoblots from different preparations). The Newman-Keuls test was performed to test the significance of differences between fractions: *$p < 0,05$ vs. other fractions °$p < 0,05$ vs. other fractions.

Europe PMC Funders Author Manuscripts

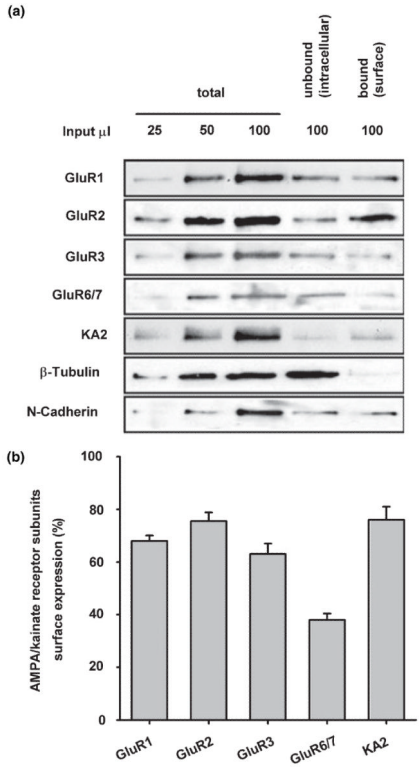

Fig. 4.

AMPAR and KAR subunit surface expression in synaptosomes. Slices containing cortex and hippocampus from adult male Wistar rats were biotinylated and the surface expression of each subunit determined by quantitative immunoblotting (see *Materials and methods*). (a) Representative blots for GluR1, GluR2, GluR3, GluR6/7, KA2, β-tubulin, N-Cadherin. (b) Cumulative plot of surface expression (mean ± SEM of three independent experiments).

Europe PMC Funders Author Manuscripts

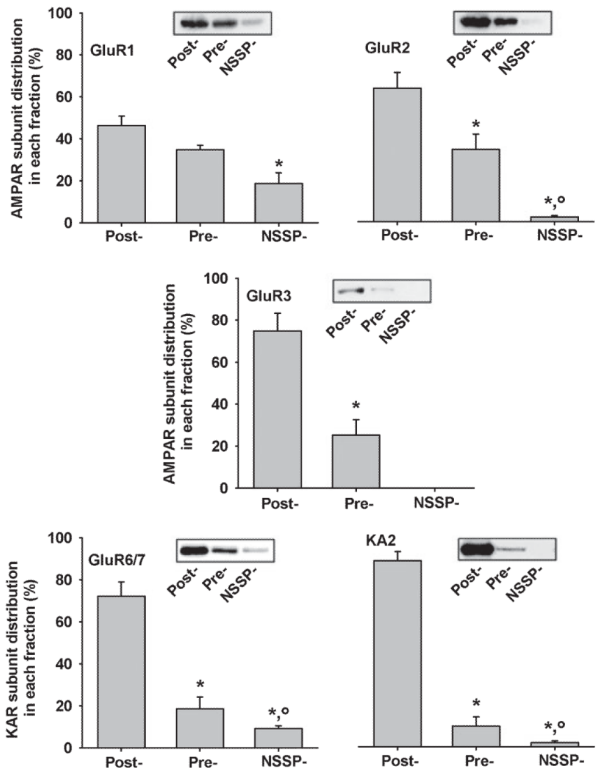

Fig. 5.

Ultrasynaptic distribution of AMPAR and KAR subunits. GluR1, GluR2, GluR3, GluR6/7 and KA2 antibodies were used. The data were normalised by adding together the density value of the band for each fraction for each antibody for each experiment (post + pre + NSSP = 100%). The data are expressed as mean ± SEM of these normalised values ($n = 3$). The Newman-Keuls test was performed to value differences between fractions: *$p < 0,05$ vs. other fractions °$p < 0,05$ vs. other fractions.

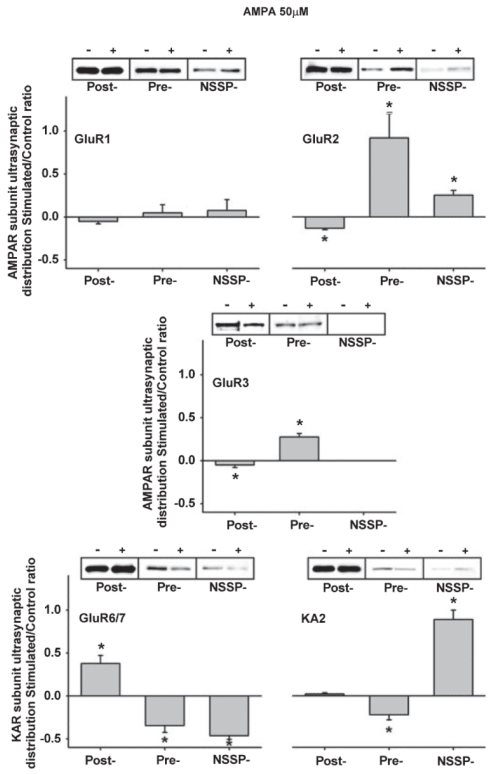

Fig. 6.

AMPA (50 μM) alters the ultrasynaptic distribution of AMPAR and KAR subunits. For both control and treated conditions the data were normalised (post + pre + NSSP = 100%) and then added together. The immunoblot panels show representative immunoreactive bands from not treated control (−) and AMPA treated (+) synaptosomes. The effect of AMPA is expressed as the ratio between the treated and the corresponding control fraction. Data are expressed as mean ± SEM values of at least three independent experiments. *$p < 0,05$ vs. control.

Europe PMC Funders Author Manuscripts

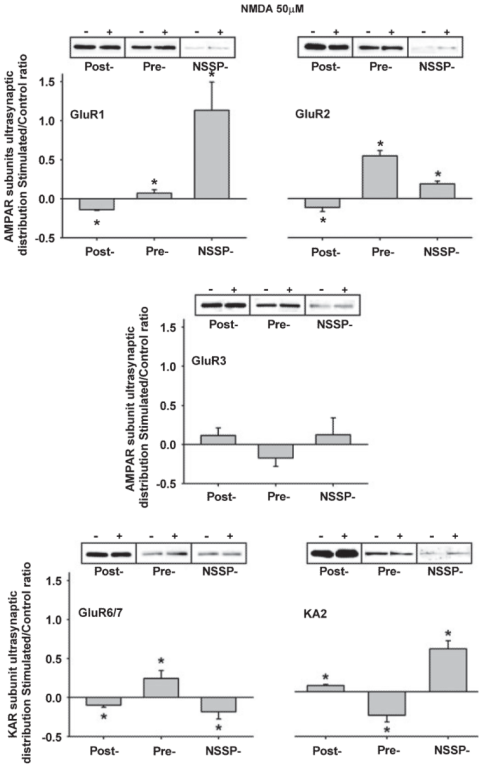

Fig. 7.

NMDA (50 μM) alters the ultrasynaptic distribution of AMPAR and KAR subunits. For both control and treated conditions the data were normalised (post + pre + NSSP = 100%) and then added together. The immunoblot panels show representative immunoreactive bands from not treated control (−) and NMDA treated (+) synaptosomes. The effect of NMDA is expressed as ratio between the treated and the corresponding control fraction. Data are expressed as mean ± SEM values of at least three independent experiments. *$p < 0,05$ vs. control.

Europe PMC Funders Author Manuscripts

Europe PMC Funders Author Manuscripts

Table 1

Summary of AMPA and NMDA effects on subunit distributions

	Postsynaptic	Presynaptic	NSSP	
GluR1	↔ (95 ± 3)	↔ (105 ±9)	↔ (108 ± 12)	
GluR2	↓ (87 ± 2)	↑ (192 ±28)	↑ (125 ±5)	
GluR3	↓ (95 ± 3)	↑ (128 ±4)	-	**AMPA**
GluR6/7	↑ (138 ±9)	↓ (66 ± 8)	↓ (54 ± 4)	
KA2	↔ (102 ±2)	↓ (78 ± 6)	↑ (189 ± 11)	

	Postsynaptic	Presynaptic	NSSP	
GluR1	↓ (86 ± 1)	↑ (107 ±5)	↑ (213 ±36)	
GluR2	↓ (88 ± 5)	↑ (155 ±7)	↑ (119 ±4)	
GluR3	↔ (111 ± 10)	↓ (83 ± 11)	↔ (112 ±22)	**NMDA**
GluR6/7	↓ (90 ± 3)	↑ (125 ± 10)	↓ (82 ± 9)	
KA2	↑ (108 ±2)	↓ (68 ± 9)	↑ (158 ±11)	